Synthesis of Sparse Linear Arrays with Tensor Decomposition

Yangjingzhi Zhuang*[1], *Yuxin Xu*[1], *Xuejing Zhang*[1*], *Zishu He*[1], *Ziwei Wang*[2], *Hongfei Yang*[3], *Lili He*[3]

[1] *University of Electronic Science and Technology of China, Chengdu, China*
[2] *Beijing institute of Control and Electronics Technology, Beijing, China*
[3] *Jiangnan Institute of Mechanical and Electrical Design, Guiyang, China*
* *zhangxuejing@uestc.edu.cn*

Keywords: SPARSE LINEAR ARRAY, MULTIPLE BEAMPATTERNS, TENSOR, HIGHER-ORDER SINGULAR VALUE.

Abstract

In this paper, tensors are innovatively applied to array optimization. Thus, an algorithm for synthesis of sparse linear arrays with multi-beampattern is proposed. Different from the traditional matrix pencil method (MPM), the proposed algorithm arranges the data obtained from the desired beampatterns into tensor form. Then a low-rank approximation is performed on this data tensor to obtain a new low-rank tensor, which is decomposed by higher-order singular value (HOSVD). By employing rotation invariance, we determine the element position of sparse array. Finally, the least square method is used to obtain the excitations corresponding to the new array, and the desired beampatterns are synthesized. Compared to MPM, our method accelerates running time while ensuring high accuracy in synthesizing beampatterns.

1 Introduction

The synthesis of a non-uniform antenna array with as few elements as possible has considerable practical applications [1]-[4]. Sparse arrays can not only reduce costs but also simplify systems. Hence, the synthesis of such sparse arrays has received increasing attention in the past period.

Random optimization is a classic synthesis technique, including genetic algorithm (GA) [5], simulated annealing (SA) [6], particle swarm optimization (PSO) [7] and differential evolution algorithm (DE) [8], etc. However, stochastic optimization algorithms have high computational complexity, especially for large arrays. In [9], Keizer proposed an iterative fast Fourier transform algorithm, significantly reducing computational complexity. And convex optimization has also been utilized to synthesize sparse arrays in [10]. Unlike the methods mentioned above, MPM can not restrict candidate antennas to grids [11],[12], thereby increasing the degree of freedom in the arrangement of array elements. On this basis, Liu et al. proposed the forward–backward matrix pencil method (FBMPM) by improving MPM in [13]. And in [14], extended matrix pencil method (EMPM) was introduced for multi-beampattern. MPM performs sparse array synthesis by constructing Hankel matrices and using low-rank approximation. However, its computational complexity increases significantly as the number of patterns increases. Furthermore, Bayesian compression sensing (BCS) technique [15],[16] offer another approach for synthesizing sparse arrays, where candidate antennas may not be limited to grids. BCS obtains both optimal positions and optimal excitations of a new sparse array through a relevance vector machine.

With reduced memory costs and the advent of advanced technology, it has become possible to collect and store vast amounts of data for various scientific, medical, and engineering applications. The data collected usually has more than two dimensions and is stored in multi-way groups as tensors instead of matrices. Tensors have found widespread practical applications in diverse fields such as chemo-metrics [17], psychometrics [18], signal processing [19], computer vision [20]-[22], data mining [23],[24], graph analysis [25], neuroscience [26]-[28] and many more. Moreover, due to the in-depth research on tensor related technologies, such as tensor singular value decomposition [29], low-rank approximation [30], low-rank completion [31], etc., tensor has also become an efficient means of data processing.

In this paper, we propose an innovative approach that applies tensors to the synthesis of linear sparse arrays. Initially, the expected beampatterns are evenly sampled to form a tensor. Subsequently, low-rank approximation is performed on the tensor to obtain a corresponding low-rank tensor. And the lower-rank tensor actually corresponds to the approximated patterns that consists of a smaller number of antenna elements. This process determines the number of elements for the new sparse array, which equals the rank of the low-rank tensor. Next, we perform a HOSVD of the low-rank tensor (i.e., Tucker decomposition of the tensor) to obtain the factor matrix. The rotation invariance of factor matrix is then used to determine the new elements positions. Finally, the corresponding excitation coefficients are calculated by the least square method, and the desired beampatterns are synthesized. The results demonstrate that the proposed method is capable of synthesizing a sparse array that satisfies multiple desired beampatterns with an appropriate number of reconstruction array elements and less running time.

https://doi.org/10.1049/icp.2024.1351

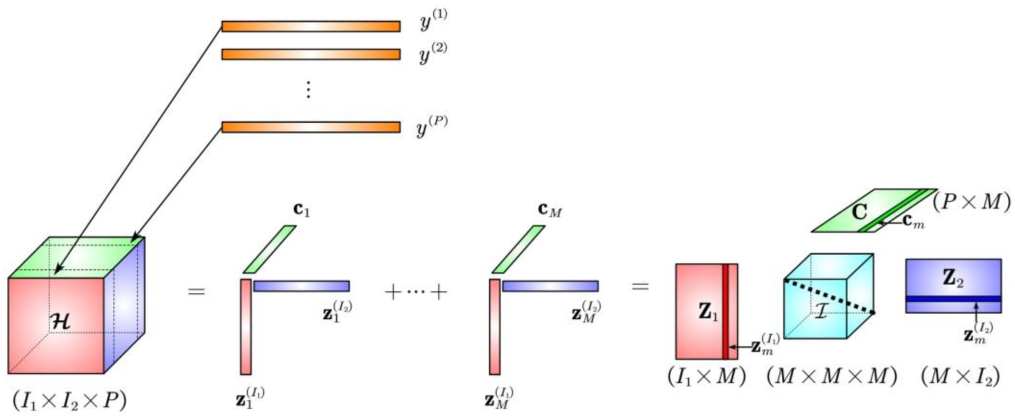

Fig. 1 Schematic diagram of the composition and decomposition of the tensor $\mathcal{H}$.

2. Sparse Array Synthesis Algorithm with Tensor

2.1 Array Model

Let a uniform linear array (ULA) be composed of M antennas. For simplicity, we assume that all antennas are isotropic. Considering P desired patterns, the p -th beampattern can be written as:

$$F^{(p)}(u)=\sum_{m=1}^{M} w_m^{(p)} e^{j\beta d_m u}, \quad p=1,2,\cdots,P \tag{1}$$

where $w_m^{(p)}$ represents the complex excitation coefficient for the p-th pattern of the m-th element, d_m stands for the distance from the m-th element to the reference element, $m=1,2,...,M$. $\beta=2\pi/\lambda$, λ is the wavelength. $j=\sqrt{-1}$ is the imaginary unit, and $u=\sin\theta$.One can see that u is defined in the domain $[-1,1]$. Sampling u uniformly:

$$u_n=n\Delta=\frac{n}{N}, \quad n=-N,\cdots,0,\cdots,N \tag{2}$$

where the number of samples is $L=(2N+1)$, and $\Delta=\dfrac{1}{N}$ is the sampling interval. Due to the Nyquist sampling theorem, the condition that $\Delta\leq \text{lambda}/(2d_{max})$ must be satisfied, where $d_{max}=\max\{d_1,...,d_M\}$. For example, for an array having M elements with a uniform spacing of $\lambda/2$, the sampling interval Δ should satisfy $\Delta\leq 1/(M-1)$, which indicates that $N\geq(M-1)$. Hence, the response of each sampling point can be expressed as:

$$\begin{aligned}\tilde{y}^{(p)}(n)&=F^{(p)}(u)|_{u=n\Delta}\\&=\sum_{m=1}^{M} w_m^{(p)} e^{j\frac{2\pi}{\lambda}d_m n\Delta}\\&=\sum_{m=1}^{M} w_m^{(p)} z_m^{n}, \quad n=-N,\cdots,0,\cdots,N\end{aligned} \tag{3}$$

where $z_m=e^{j\frac{2\pi}{\lambda}d_m\Delta}$. And we consider the following vector:

$$\begin{bmatrix}\tilde{y}^{(p)}(-N)\\ \tilde{y}^{(p)}(-N+1)\\ \vdots\\ \tilde{y}^{(p)}(N-1)\\ \tilde{y}^{(p)}(N)\end{bmatrix}=\begin{bmatrix}\sum_{m=1}^{M} w_m^{(p)} z_m^{-N}\\ \sum_{m=1}^{M} w_m^{(p)} z_m^{-N+1}\\ \vdots\\ \sum_{m=1}^{M} w_m^{(p)} z_m^{N-1}\\ \sum_{m=1}^{M} w_m^{(p)} z_m^{N}\end{bmatrix}=\begin{bmatrix}1&1&\cdots&1\\ z_1&z_2&\cdots&z_M\\ z_1^2&z_2^2&\cdots&z_M^2\\ \vdots&\vdots&\ddots&\vdots\\ z_1^{2N}&z_2^{2N}&\cdots&z_M^{2N}\end{bmatrix}\begin{bmatrix}w_1^{(p)} z_1^{-N}\\ w_2^{(p)} z_2^{-N}\\ \vdots\\ w_M^{(p)} z_M^{-N}\end{bmatrix} \tag{4}$$

Let $y_l^{(p)}=\tilde{y}^{(p)}(l-N)$, $l=0,1,\cdots,2N$, and the constructed tensor $\mathcal{H}\in\mathbb{C}^{I_1\times I_2\times P}$ is as follows:

$$[\mathcal{H}]_{i_1,i_2,i_3}=y_{i_1+i_2-1}^{(i_3)} \tag{5}$$

where $i_1=1,\cdots,I_1, i_2=1,\cdots,I_2, i_3=1,\cdots,P$. And $I_1+I_2-1=2N+1$.

$$[\mathcal{H}]_{i_1,i_2,i_3}=\sum_{m=1}^{M} c_m^{(i_3)}\cdot(z_m^{i_1-1}\cdot z_m^{i_2-1}) \tag{6}$$

where $c_m^{(p)}=w_m^{(p)} z_m^{-N}$. Thus, the tensor $\mathcal{H}$ can be represented as follows:

$$\mathcal{H}=\sum_{m=1}^{M} 1\cdot \boldsymbol{z}_m^{(I_1)}\circ \boldsymbol{z}_m^{(I_2)}\circ \boldsymbol{c}_m \tag{7}$$

where $\circ$ represents outer product operation, and $\boldsymbol{c}_m=[c_m^{(1)},c_m^{(2)},\cdots,c_m^{(P)}]^T$. $\boldsymbol{z}_m^{(I_1)}=[1,z_m,z_m^2,\cdots,z_m^{I_1-1}]^T$ and $\boldsymbol{z}_m^{(I_2)}=[1,z_m,z_m^2,\cdots,z_m^{I_2-1}]^T$. Hence, we can write the tensor $\mathcal{H}$ as

$$\mathcal{H}=\mathcal{I}\times_1 \boldsymbol{Z}_1\times_2 \boldsymbol{Z}_2\times_3 \boldsymbol{C} \tag{8}$$

where $\mathcal{I}$ is a core tensor of size $M\times M\times M$ with hyperdiagonal structure and diagonal element 1. And

$\boldsymbol{Z}_1 = \left[\boldsymbol{z}_1^{(I_1)}, \cdots, \boldsymbol{z}_M^{(I_1)}\right] \in \mathbb{C}^{I_1 \times M}$, $\boldsymbol{Z}_2 = \left[\boldsymbol{z}_1^{(I_2)}, \cdots, \boldsymbol{z}_M^{(I_2)}\right] \in \mathbb{C}^{I_2 \times M}$, $\boldsymbol{C} = [\boldsymbol{c}_1, \cdots, \boldsymbol{c}_M] \in \mathbb{C}^{P \times M}$. The symbol $\times_i$ stands for the i-mode product operation. The arrangement of sampled data and the composition and decomposition of the tensor are illustrated in Fig 1.

2.2 Synthesis of Sparse Array

In this subsection, the tucker decomposition of tensors needs to be introduced first. Tucker decomposition, also known as higher-order singular value decomposition, is a multi-linear extension of SVD. Tucker decomposition represents a given tensor as a combination of a kernel tensor multiplied by a factor matrix along each mode in order to represent the associated information of each mode subspace and the inherent structure information of data. Hence, the Tucker decomposition of the tensor $\mathcal{H}$ is carried out as:

$$\mathcal{H} = \mathcal{G} \times_1 \boldsymbol{U}^{(1)} \times_2 \boldsymbol{U}^{(2)} \times_3 \boldsymbol{U}^{(3)} \tag{9}$$

where $\mathcal{G}$ is the core tensor size of $M \times M \times M$. Different from singular value matrix, the core tensor does not take diagonal structure and is generally a full tensor, that is, its non-diagonal elements are usually not equal to zero. The factor matrix $\boldsymbol{U}^{(i)}$ requires the orthogonal column structure similar to the left singular matrix and unitary matrix of SVD, that is, any two columns of $\boldsymbol{U}^{(i)}$ are mutually orthogonal. $\boldsymbol{U}^{(i)}$ and $\boldsymbol{Z}_i$ correspond to the same column space.

In addition, if the number of samples is large enough, the rank of the tensor is equal to the number of elements. If we want to reduce the number of array elements, an approximation error ε can be added when conducting HOSVD, so as to obtain a low-rank approximation decomposition result:

$$\begin{aligned} &\mathcal{H} \approx \tilde{\mathcal{G}} \times_1 \tilde{\boldsymbol{U}}^{(1)} \times_2 \tilde{\boldsymbol{U}}^{(2)} \times_3 \tilde{\boldsymbol{U}}^{(3)} \\ &s.t. \quad \| \mathcal{H} - \tilde{\mathcal{G}} \times_1 \tilde{\boldsymbol{U}}^{(1)} \times_2 \tilde{\boldsymbol{U}}^{(2)} \times_3 \tilde{\boldsymbol{U}}^{(3)} \|_F \leq \varepsilon \end{aligned} \tag{10}$$

where $\|\cdot\|_F$ is Frobenius norm. So, we have:

$$\tilde{\boldsymbol{U}}^{(1)} = \boldsymbol{Z}_1 \boldsymbol{Q} \tag{11}$$

where $\boldsymbol{Q}$ is a non-singular matrix. In the case of tensors, from the structure of $\boldsymbol{Z}_1$, we are not hard to see that it satisfies a particular rotational invariance:

$$\boldsymbol{Z}_{1,l} \boldsymbol{\Psi} = \boldsymbol{Z}_{1,f} \tag{12}$$

where $\boldsymbol{\Psi} = \mathrm{diag}(z_1, \cdots, z_M)$, $\boldsymbol{Z}_{1,l}$ and $\boldsymbol{Z}_{1,f}$ are obtained by removing the last and first row of $\boldsymbol{Z}_1$, respectively. By combining (11) and (12), the following equation can be derived:

$$\tilde{\boldsymbol{U}}_l^{(1)} \overline{\boldsymbol{\Psi}} = \tilde{\boldsymbol{U}}_f^{(1)} \tag{13}$$

where $\overline{\boldsymbol{\Psi}} = \boldsymbol{Q}^{-1} \boldsymbol{\Psi} \boldsymbol{Q}$, $\tilde{\boldsymbol{U}}_l^{(1)}$ and $\tilde{\boldsymbol{U}}_f^{(1)}$ are obtained by removing the last and first row of $\tilde{\boldsymbol{U}}^{(1)}$, respectively. From (13) we can find matrix $\overline{\boldsymbol{\Psi}}$, and then perform SVD on the matrix to obtain the eigenvalues $\gamma_g, g = 1, \cdots, G$ and $G \leq M$. So, there is

$$\gamma_g = \widehat{z}_g = e^{-j\frac{2\pi}{\lambda}\widehat{d}_g \Delta} \tag{14}$$

Therefore, by Eq. (14), we can calculate the element positions of the new sparse array. Finally, the corresponding excitations are solved by the least squares method:

$$\boldsymbol{W}_{new} = (\boldsymbol{A}_{new}^T \boldsymbol{A}_{new})^{-1} \boldsymbol{A}_{new}^T \boldsymbol{Y} \tag{15}$$

where $\boldsymbol{A}_{new}$ is the array manifold of the new sparse array and $\boldsymbol{Y} = [\boldsymbol{y}^{(1)}, \ldots, \boldsymbol{y}^{(P)}]$.

3 Simulations

In this section, representative simulations are carried out to validate the proposed method. For comparison purpose, the EMPM in [14] is also tested.

In the first situation, we consider a ULA of $M = 60$ isotropic elements spaced by half wavelength. We selected $P = 13$ beampatterns, whose mainlobe directions change uniformly at 2° intervals in $[\theta_0 | \theta_0 \in [-12^\circ, 12^\circ]$, and the sidelobe levels are all constrained to below -30dB. The simulation results are shown in Fig 2 and Fig 4.

We set the number of new elements to 43 for both the proposed method and EMPM. The low rank approximation error of the proposed method is 10^{-7}, while which of EMPM is 10^{-9}. The distribution of new and initial elements is demonstrated in the Fig 2, and it can be observed that the arrays obtained by both methods are non-uniform and the elements are not restricted to the original positions. The apertures of new arrays obtained by the proposed algorithm and EMPM both are 29.50λ. The beampatterns synthesized by new and initial arrays are displayed in the Fig 4, and we can observe that the final synthesized beampatterns of the two methods can meet the requirements well, except that the synthesized beampattern of EMPM has slightly higher sidelobe levels near 90° and -90°.

In the second situation, a ULA of $M = 56$ isotropic elements spaced by half wavelength is considered. We selected $P = 11$ beampatterns with mainlobe directions changing uniformly at 2° intervals in $[\theta_0 | \theta_0 \in [-10^\circ, 10^\circ]$. In particular, the level of a notch at $[40^\circ, 55^\circ]$ in the sidelobe is limited to less than -40dB, while all the other sidelobe levels are below -20dB. The simulation results are shown in Fig 3 and Fig 5.

The new array consists of 40 elements. The proposed method still sets the low rank approximation error to 10^{-7}, while that of EMPM is 10^{-9}. In Fig 3, the distribution of new and initial elements is demonstrated. It can be seen that the array obtained by the two methods are not uniform, and the distribution of elements is not limited by the original element

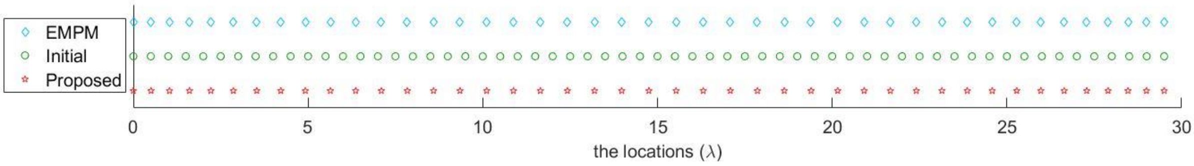

Fig. 2 Comparison of the positions of the new and initial elements.

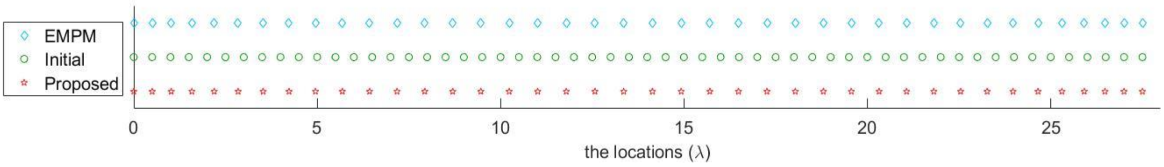

Fig 3. Comparison of the positions of the new and initial elements.

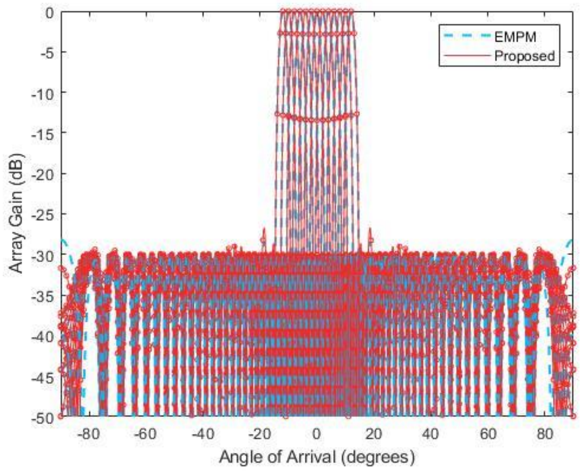

Fig 4. Comparison of the beampattern of the new and initial array.

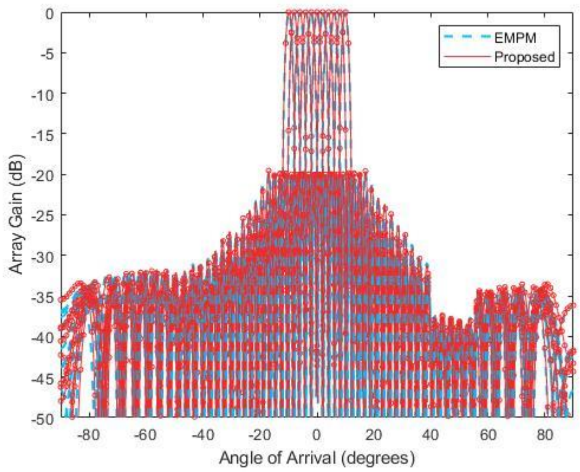

Fig 5. Comparison of the beampattern of the new and initial array.

positions. The apertures of new arrays obtained by the proposed algorithm and EMPM are both 29.50 λ . And beampatterns synthesized by new and initial arrays are displayed in the Fig 5. The sidelobe levels of the synthesized beampatterns are lower than -20dB, but the sidelobe levels at the notch are slightly higher than -40dB. To sum up, both methods are effective.

The running time of the proposed method and EMPM with different parameter settings are presented in Table 1. Overall, it can be concluded that the proposed method is faster than EMPM, making it more efficient for practical and applications. In addition, the computation time of EMPM varies significantly with the chosen parameters, but the proposed method consistently maintains a fast computation speed.

Table 1 Comparison of running time.

Parameter setting	proposed method	EMPM
M=20, P=13	0.03s	0.06s
M=20, P=81	0.04s	0.53s
M=60, P=13	0.12s	0.35s
M=60, P=81	0.20s	11.48s
M=100, P=13	0.14s	0.54s
M=100, P=81	0.63s	19.97s
M=150, P=81	1.14s	61.02s
M=150, P=151	1.72s	216.51s

4 Conclusion

In this paper, we have introduced a novel sparse array synthesis algorithm by utilizing tensors in array optimization. Specifically, transformed the sampled data of the reference beampatterns into a tensor and then performed a low-rank approximation to obtain a low-rank tensor. Then the low-rank tensor was decomposed by HOSVD to get the element positions and excitations of the new sparse array. The simulation results of two scenarios have demonstrated the effectiveness of the proposed algorithm in synthesizing sparse arrays that meet the requirements of multi-beampattern. Notably, our proposed algorithm outperforms EMPM in terms of running time, particularly when the number of elements and beampatterns increase.

5 Acknowledgements

This work was supported in part by the National Nature Science Foundation of China under Grant 62101101, and the Peng Cheng Shang Xue Education Fund of UESTC Education Development Foundation under Grant XY2021602.

6 References

[1] C. A. Balanis: 'Antenna Theory: Analysis and Design'. (Wiley Press, 3rd edn. 2005)

[2] G. K. Mahanti, S. Das, and A. Chakraborty: 'Design of phase-differentiated reconfigurable array antennas with minimum dynamic range ratio', IEEE Antennas Wireless Propag. Lett., 2006, 5, pp 262–264

[3] R. Vescovo: 'Reconfigurability and beam scanning with phase-only control for antenna arrays', IEEE Trans. Antennas Propag., 2008, 56, (6), pp 1555–1565

[4] A. F. Morabito, A. Massa, P. Rocca, et al.: 'An effective approach to the synthesis of phase-only reconfigurable linear arrays ', IEEE Trans. Antennas Propag., 2012, 60, (8), pp 3622–3631

[5] R. L. Haupt: 'Thinned arrays using genetic algorithms', IEEE Trans. Antennas Propag., 1994, 42, (7), pp 993-999

[6] V. Murino, A. Trucco, and C. S. Regazzoni: 'Synthesis of equally spaced arrays by simulated annealing', IEEE Trans. Signal Process., 1996, 44, (1), pp 119-122

[7] D. W. Boeringer, D. H. Werner: 'Particle swarm optimization versus genetic algorithms for phased array synthesis', IEEE Trans. Antennas Propag., 2004, 52, (3), pp 771-779

[8] S. Caorsi, A. Massa, M. Pastorino, et al.: 'Optimization of the difference patterns for monopulse antennas by a hybrid real/integercoded differential evolution method', IEEE Trans. Antennas Propag., 2005, 53, (1), pp 372-376

[9] W. P. M. N. Keizer: 'Linear array thinning using iterative FFT techniques', IEEE Trans. Signal Process., 2008, 56, (8), pp 2757-2760

[10] S. E. Nai, W. Ser, Z. L. Yu, et al.: 'Beam pattern synthesis for linear and planar arrays with antenna selection by convex optimization', IEEE Trans. Antennas Propag., 2010, 58, (12), pp 3923-3930

[11] Y. Hua and T. K. Sarkar: 'Matrix pencil method for estimating parameters of exponentially damped/undamped sinusoids in noise', IEEE Trans. Antennas Propag., 1990, 38, (5), pp 814–824

[12] Y. Liu, Z. Nie, and Q. H. Liu: 'Reducing the number of elements in a linear antenna array by the matrix pencil method', IEEE Trans. Antennas Propag., 2008, 56, (9), pp 2955–2962

[13] Y. Liu, Q. H. Liu, and Z. Nie: 'Reducing the number of elements in the synthesis of shaped-beam patterns by the forward-backward matrix pencil method', IEEE Trans. Antennas Propag., 2010, 58, (2), pp 604–608

[14] Y. Liu, Q. H. Liu, and Z. Nie: 'Reducing the number of elements in multiple-pattern linear arrays by the extended matrix pencil methods', IEEE Trans. Antennas Propag., 2014, 62, (2), pp 652–660

[15] G. Oliveri, A. Massa: 'Bayesian compressive sampling for pattern synthesis with maximally sparse non-uniform linear arrays', IEEE Trans. Antennas Propag., 2011, 59, (2), pp 467-481

[16] G. Oliveri, M. Carlin, and A. Massa: 'Complex-weight sparse linear array synthesis by Bayesian compressive sampling', IEEE Trans. Antennas Propag., 2012, 60, (5), pp 2309-2326

[17] A. Smilde, R. Bro, P. Geladi: 'Multi-way Analysis: Applications in the Chemical Sciences'. (Wiley Press, 2004)

[18] P. Kroonenberg: 'Three-mode Principal Component Analysis: Theory and Applications'. (Leiden Press, 1983)

[19] J. G. McWhirter, I. K. Proudler: 'Mathematics in Signal Processing V'. (Oxford Press, 2002)

[20] M. Vasilescu, D. Terzopoulos: 'Multilinear analysis of image ensembles: tensorfaces'. Proc. ECCV, Copenhagen, Denmark, May 2002, pp. 447-460

[21] M. Vasilescu, D. Terzopoulos: 'Multilinear image analysis for facial recognition'. Proc. ICPR, Quebec City, QC, Canada, August 2002, pp. 511–514

[22] M. Vasilescu, D. Terzopoulos: 'Multilinear subspace analysis of image ensembles'. Proc. CVPR, Madison, WI, USA, June 2003, pp. 93–99

[23] E. Acar, S. Cantele, M. Krishnamoorth, et al.: 'Modeling and multiway analysis of chatroom tensors'. Proc. EMBS, Shanghai, China, September 2005, pp. 256–268

[24] B. Savas, L. Eldon: 'Handwritten digit classification using higher order singular value decomposition', Pattern Recognit., 2007, 40, (3), pp 993–1003

[25] T. Kolda, B. Bader: 'Higher-order web link analysis using multilinear algebra'. Proc. ICDM, Houston, TX, USA, November 2005, pp. 242–249

[26] C. Beckmann, S. Smith: 'Tensorial extensions of the independent component analysis for multisubject FMRI analysis', NeuroImage, 2005, 25, (1), pp 294–311

[27] F. Miwakeichi, E. Martínez-Montes, P. Valdés-Sosa, et al.: 'Decomposing EEG data into space–time–frequency components using parallel factor analysis', NeuroImage 2004, 22, (3), pp 1035–1045

[28] J. Nagy, M. Kilmer: 'Kronecker product approximation for preconditioning in three-dimensional imaging applications', IEEE Trans. Image Process., 2006, 15,(3), pp 604–613

[29] M. E. Kilmer, C. D. Martin: 'Factorization strategies for third-order tensors- ScienceDirect', Linear Algebra and its Applications, 2011, 435, (3), pp 641-658

[30] M. Ishteva, P.-A. Absil, S. Van Huffel, et al.: 'Best low multilinear rank approximation of higher-order tensors, based

on the Riemannian trust-region scheme', SIAM Journal on Matrix Analysis and Applications, 2011, 32, (1), pp 115–135
[31] C. Lu, X. Peng, and Y. Wei: 'Low-rank tensor completion with a new tensor nuclear norm induced by invertible linear transforms'. Proc. CVPR, Long Beach, CA, USA, June 2019, pp. 5996-6004